

# Total Dose Effects on Microelectromechanical Systems (MEMS): Accelerometers\*

C. I. Lee, A. J. Johnston, W. C. Tang, and C. E. Barnes  
Jet Propulsion Laboratory  
California Institute of Technology  
Pasadena, CA

J. Lyke  
Philips Laboratory  
Kirtland Air Force Base, NM

## Abstract

Microelectromechanical sensors, ADXL50 and XMMAS40G accelerometers which are fabricated with surface micromachining techniques are characterized for total dose radiation. An unusual failure mechanism that appears to be associated with the sensor was observed and presented in this paper.

## I. Introduction

Microelectromechanical systems (MEMS) are new technologies with a wide range of applications; automotive, biomedical instrumentation, and scientific. It is a technology that combines electronics and micromechanical devices in one package. The growth of MEMS has attracted a broad range of research and industry interests. The most important application of MEMS, so far, is in the microsensor area, such as pressure sensors, chemical sensors, and accelerometers.

MEMS technology is particularly attractive to space systems. It promises to play a crucial role in future miniaturized spacecraft, such as those planned by New Millennium Program. This paper presents total dose test results for two MEMS accelerometers, Analog Devices ADXL50 and Motorola

XMMAS40G.

## II. Device Descriptions

The analog device ADXL50 is a microelectromechanical sensor which measures up to  $\pm 50$  g acceleration on a single monolithic integrated circuit. As shown in Figure 1, it contains a polysilicon surface-micro machined sensor and signal conditioning circuitry. It uses a differential capacitor sensor consisting of independent fixed plates and a movable floating central plate which deflects in response to changes in relative motion. The sensor element and electronic circuitry were fabricated with a BiCMOS process. The acceleration sensor contains 42 unit cells and a common beam. Figure 2 is a scanning electron microscope (SEM) picture of the ADXL50 sensor at rest (0 g). The outer two capacitors are series connected, forming a capacitive divider with a common movable central plate. When an acceleration is applied, the common central plate (beam) moves closer to one of the fixed plates while moving further from the other. The output amplitude increases with the amount of acceleration applied at the sensor.

External resistors were used to set the gain and offset of the internal buffer amplifier to provide 1.5 V to 3.5 V full scale output range. The device sensitivity is 19 mV/g and the full scale output swing is  $\pm 0.95$  volts for  $\pm 50$  g acceleration. The zero g

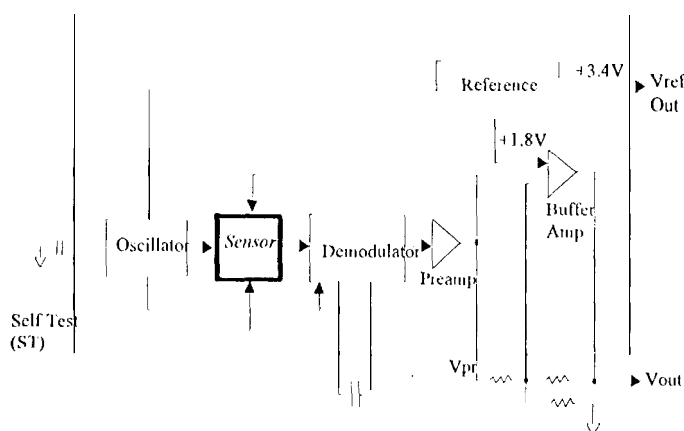


Figure 1. Functional block diagram of ADXL50.

The work described in this paper was carried out by the Jet Propulsion Laboratory, California Institute of Technology, under contract with the National Aeronautics and Space Administration Code Q. Work funded by the NASA Microelectronics Space Radiation Effects Program (MSREP).

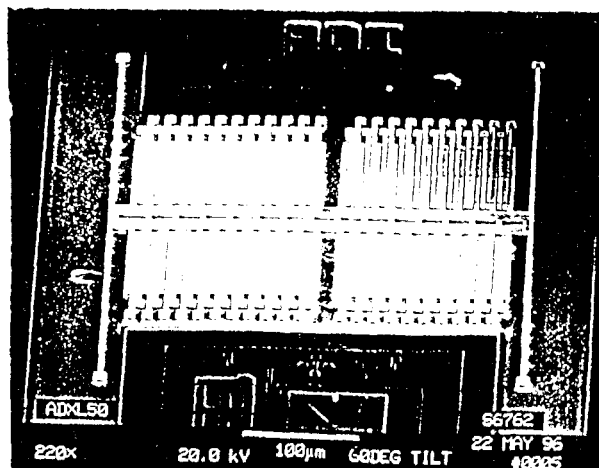


Figure 2. A SEM photograph of the sensor at rest,

- output level of the pre-amplifier ( $V_{pr}$ ) is -11.8 volts.

Motorola XMMAS40G is a silicon capacitive, micro-machined accelerometer. It consists of a single polysilicon seismic mass which suspends between two fixed polysilicon plates (G-Cell). The (i-cell is scaled at the die level, creating a particle-free environment. The full-scale measurement is  $\pm 40$  g and the sensitivity of the device is 35 mV/g. The device is fabricated with a commercial CMOS process.

#### III. Test Setup

A special test set-up employing a variable speed rotating arm was fabricated using a slip-ring assembly, dc motor, and other equipment to measure the linearity of the sensitivity of the accelerometer. The device under test was located at one end of a 10" rotating arm. The output voltage, reference voltage, and  $V_{pr}$  were measured at various acceleration levels with an HP3458A precision DMM. Negative g levels can be measured by changing the device orientation 180° at the end of the 10" arm. A detailed diagram of the test apparatus will be included in the final paper.

#### IV. Test Results

##### a) Analog Devices ADXL50

##### Cobalt-60 Test Results

Devices were irradiated at a dose rate of 25 rad(Si)/s in a static (non-rotating) condition. At levels between 5 and 20 krad(Si) the device continued to operate normally, with a slight shift in output voltage and slope. At higher levels, an unusual failure mode developed, as shown in Figure 3. The output voltage was initially stuck at a low voltage (50 mV). It remained stuck when the device was accelerated to g-levels below 30 g. However, normal operation could be restored by accelerating them to a sufficient high g-level (approximately 30 g). When devices remained functional from -50 g level to 50 g level as long as the device power supply was on. However, once the power supply voltage was removed, the output voltage reverted to the stuck mode. Normal operation could again be restored by

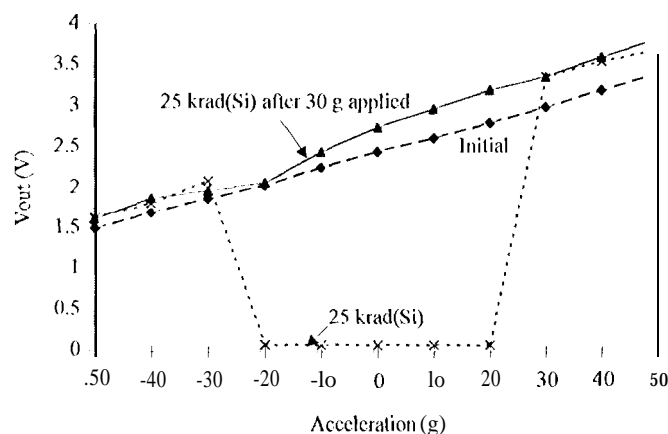


Figure 3. ADXL50 HDR [25 rad(Si)/s] test result.

accelerating the device to 30 g, but the device always returned the stuck mode once power was removed.

As shown in Figure 1, the pin configuration of this circuit allows separate measurements of the buffer amplifier. Input offset voltage, input bias current, and output voltage of the output buffer amplifier were measured, but insignificant degradation was observed during irradiation. The 3.4 V reference voltage showed no degradation at all.

Electrical parameters of irradiated devices did not show any indication of annealing after 24 hours at room temperature, after they were irradiated to 25 krad(Si). However, a device recovered fully after 144 hours at 100 °C. This device was irradiated further to observe the failure mechanism at higher total dose level. The device was functional until it was exposed to an additional 15 krad(Si), 40 krad(Si) total. It failed similarly as before, but in this case it recovered within 1 hour at room temperature annealing. The other device was subjected to 168 hour of 100 °C annealing period to observe any rebound effects. However, no rebound was observed. The annealing test results imply that this BiCMOS accelerometer should withstand much higher total dose irradiation at a low dose rate, and low dose-rate tests are in progress. They will be included in the final paper.

A static functional test was performed using the self-test function. This test can be used to verify the functionality of the device statically when the dynamic linearity test system is not available. When logic high voltage is applied to the self-test input, an electrostatic force is applied to the sensor so that the sensor will be in the negative full-scale output state (-50 g level). A correctly functioning accelerometer will respond by initiating about -1 volt output change at  $V_{pr}$ . The output will return to 0 g level when the self test input level goes low. Figure 4 shows test results of a control device and irradiated devices at 25 krad(Si) using the self test function. The plot of  $V_{pr}$  and  $V_{out}$  of the control device (dotted line in Figure 4) indicates that the device functions properly.  $V_{pr}$  of irradiated devices degraded significantly after 20 krad(Si). However, they still responded to applied voltage at the self-test input. The output of one device (solid line in Figure 4) shows a partial functionality when the

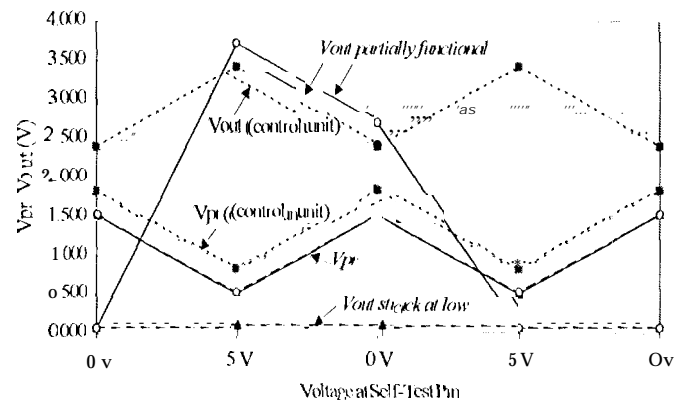


Figure 4. Self-test functional test of control unit and two failed devices; one device was partially functional; the other device was stuck low.

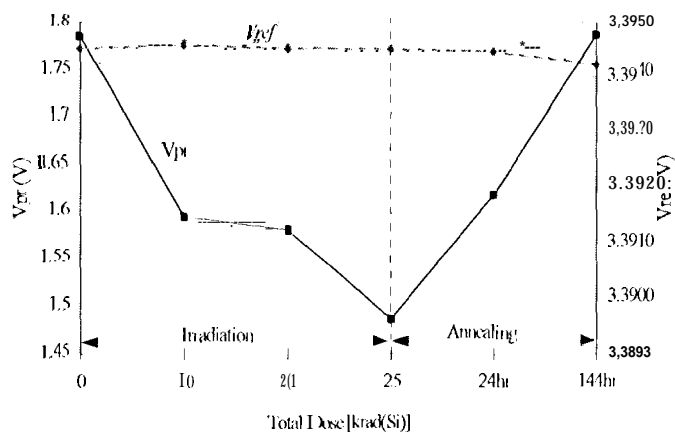


Figure 5. ADXL50 Vpr and Vref degradation

self-test input is high (5 V), but it was non functional when the self test input is low (0 V). The output of another device stuck at low (dashed line in Figure 4) and did not respond to the self-test input at all at 25 krad(Si).

The internal reference voltage and the buffer amplifier showed insignificant degradation during total dose irradiation. However, the output voltage of the pre-amplifier,  $V_{pr}$ , degraded significantly with radiation and showed rapid annealing after high-temperature annealing period, although it did not anneal at room temperature. It is shown in Figure 5. Note that the pre-amplifier and the output buffer amplifier are identical op-amps. It is clear that when  $V_{pr}$  degrades and reaches a certain value, below 1.5 V, then the device is non functional. The 3.4 V reference voltage output changed less than 1 mV after irradiation, as shown in Figure 5,

After high temperature annealing,  $V_{pr}$  values recovered to the initial values and devices functioned properly. This annealing behavior indicates that electronic circuit degradation caused the  $V_{pr}$ -related failure after irradiation rather than the electro-mechanical element.

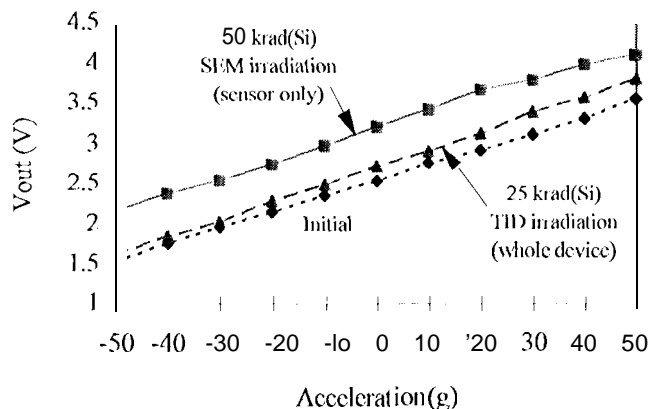


Figure 6. Results with SEM localized irradiation [50 krad(Si)] at sensor

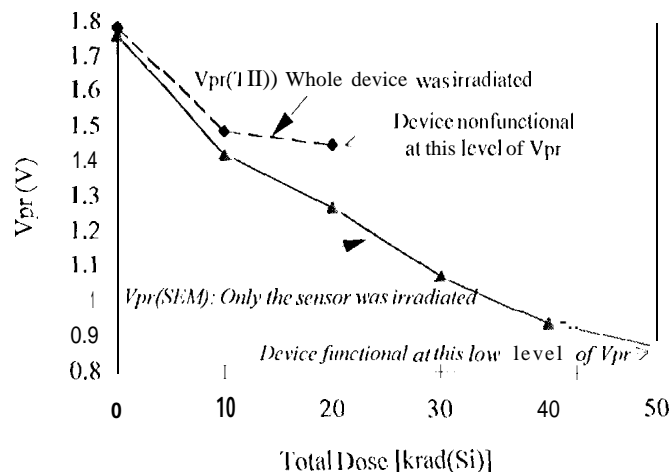


Figure 7. Comparison of results with whole-chip and localized irradiation of the sensor.

### SEM Irradiation Result

A SEM irradiation technique was used to irradiate only the sensor portion of the ADXL50 using a method previously developed [2-4]. The dose rate of 1 krad(Si)/s was calculated based on the area of the sensor which was to be irradiated and beam current was set accordingly with the 30 KcV beam voltage. (Details will be included in the final paper.)

The linearity curve of the device did not show any nonlinearities up to the dose level of 50 krad(Si). However, it showed offset errors, in other words, the curve shifted up along the y-axis as in Figure 6. Note that the hysteresis like response when the whole device was irradiated as shown in Figure 3 was not observed when the only sensor was irradiated. The linearity curve shifted up to the final dose level of 50 krad(Si).

$V_{pr}$  also showed significant degradation during SEM irradiation and it is shown in Figure 7.  $V_{pr}$  changed from 1.765 V initial value to 0.826 V at 50 krad(Si) and the device was still functional at the low value of  $V_{pr}$  unlike the total dose test results when the whole device was irradiated. After 50 krad(Si) of SEM irradiation, the  $V_{pr}$  was less than 1 V which means that the self test function would fail at this level of radial ion.  $V_{pr}$  of 0.826 V changed to 0.132 V when a logic high is applied at the self test input, the  $V_{pr}$  should be reduced full one volt. In this case the  $V_{pr}$  reached the saturation limitation and failed the self test function test. However, the overall transfer curve of the device output still remained functional as shown in Figure 6 even though the self test function test failed.

### b) Motorola XMMAS40G Accelerometer

#### High Dose Rate Test Result

This CMOS fabricated device exhibited small changes in the output g-level response at low total dose levels, but failed functionally at 4 krad(Si). The output of the device stack at high level (4.86 V) as shown in Figure 8. Devices did not show any indication of annealing during 24 hours at room temperature.

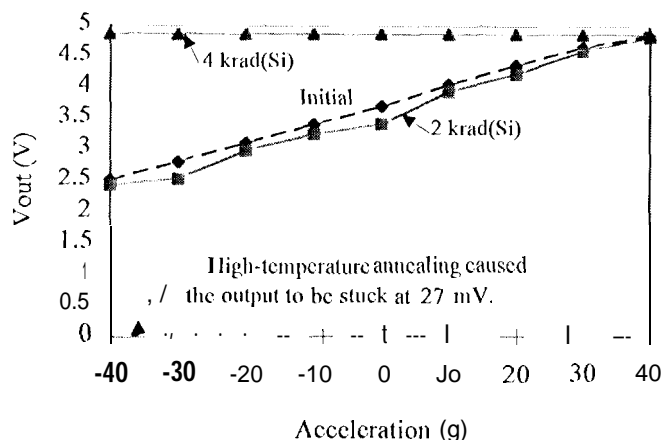


Figure 8. Motorola XMMAS40G IIR test result

However, the output changed to 2.7 mV and device was nonfunctional after 168 hours 100 °C annealing.

After the high temperature annealing test, a peculiar post-irradiation lock-up condition was observed for this device. When a device was accelerated to about 40 g level and stayed about 2.0 seconds, the output jumped back to 3.505 V which indicates that the device is nonfunctional. The supply current increased to 112 mA. The nominal supply current was about 3.5 mA throughout full scale output g-levels. Then, the power supply was removed and applied for several seconds. The output stayed at 27 mV and the supply current was 3.03 mA. The power supply was turned on and off several times to make sure the output was in stable mode. Again, the device was spun up to about 40 g level, then, the device output increased to 3.588 V and the supply current jumped up to 113.7 mA. To clear this mode, the power had to be recycled and the output returned to 27 mV.

This is an unusual failure mechanism of a CMOS device due to a combination of radiation damage and annealing. When the device is in high g-level mode, the device starts drawing tremendous amount of current and the output sticks at high level. This appears to be an effect of the micromechanical sensor and CMOS electronic components interaction. Devices were delidded for SEM analysis. None of the devices functioned after delidding. The die was too delicate to touch and none of the delidding attempts seemed to work successfully. We are in the process of getting a die sample from Motorola to analyze and the final paper will include further work on the unusual failure mode of this device.

## V. Discussion

The two microelectromechanical sensors that are discussed in the paper show unusual failure modes when they are subjected to ionizing radiation. The BiCMOS device functions at much higher radiation levels than the sensor that is fabricated with CMOS technology, although the two devices also use different sensor designs and device architectures.

Localized irradiation of the sensor element in the ADXL50 shows that the sensor is affected by radiation, as well as the peripheral electronics. This may be caused by charge build up in the plates of the sensor capacitor array. More details will be included in the final paper, along with results of irradiation at low dose rate.

The failure mode of the CMOS device was also complex, although it failed at a far lower level than the BiCMOS device. Low dose-rate tests are also in progress for this device type in order to determine if the stuck-low mechanism that was observed after high temperature annealing also occurs at low dose rate.

The key issue for these devices is to understand how the sensor technology and device architecture affect the results. Initial tests suggest that the interplay of the sensor and electronic devices affects both part types. This will be further studied for the final paper.

## VI. References

- [1]. Analog Devices Data Book, "Monolithic Accelerometer with Signal Conditioning: ADXL50".
- [2]. S. Cohen, L. Hughes, "SEM irradiation for Hardness Assurance Screening and Process Definition," IEEE Trans. Nucl. Sci. NS-21, Dec. 1974.
- [3]. C. G. Thomas, K. C. Evans, "The SEM as a Diagnostic Tool for Radiation Hardness Design of Microcircuits," Scanning Electron Microscopy, p. 978, Vol. 1.
- [4]. K. F. Galloway, P. Roitman, "Important Considerations for SEM Total Dose Testing," IEEE Trans. Nucl. Sci. NS-24, 7066 (1977).